

# Application of a two phase hydrodynamic modeling to an electrowinning cell

A. Filzwieser, K. Hein and G. Hanko  
*Department of Nonferrous Metallurgy*  
*University of Leoben*  
*A-8700 Leoben, Austria*

H. Grogger  
*AVL List GmbH*  
*A-8020 Graz, Austria*

## ABSTRACT

The highest useable current density in an electrowinning process is between 50 to 60 % of the limit current density. One of the most important influences of the limit current density is the thickness of the hydrodynamic boundary layer in front of the electrodes. Therefore, the fluid flow in a copper electrowinning cell is calculated. The numerical simulation - using the CFD-software package FIRE® - considers all three different causes of the fluid flow: natural convection, forced convection by electrolyte circulation and forced convection by electrochemically induced gas stirring. The simulation of natural convection is based on different density values in the boundary layer at the electrode's surface given by a density/concentration correlation. The copper concentration - linked with current density by the Faraday law - is solved by an additional transport equation. The simulation of the forced convection by the electrochemically induced gas stirring is done by using a real two phase calculation. That means that all differential equations are solved again for the second phase. The numerical solution of the fluid flow field is compared with results of LDA-measurements, which were done in a special cell. The software for the LDA enabled a calculation of the void fraction possible and therefore a rough estimate of the mass transfer coefficient through the prevailing gas bubble induced convection can be given, assuming influence of relative bubble volumina.

## **INTRODUCTION**

To increase the productivity of a hydro-electrical unit operation without additional costs, it is necessary to increase the current density to get more metal per time unit and area. For a good quality of metal deposition on the cathode, only 60 % of the limit current density can be used. One of the most important influences of the limit current density is the thickness of the boundary layers (hydrodynamic as well as diffusion layer) in front of the electrodes. A very important figure in this relation is the mass transport coefficient.

In the first part of the paper basic investigations and measurements concerning primarily the hydrodynamic fluid flow in a copper electrowinning cell and secondarily the benefit of the fluid flow onto the mass transport are given. Afterwards, the numerical simulation of the before used electrowinning cell is explained.

## **HYDRODYNAMIC FLUID FLOW FIELD**

In electrometallurgical cells, the fluid flow can be ascribed to natural convection, bubble stirring and to forced convection.

The following theoretical treatment of fluid flow in an aqueous electrowinning cell describes the motion of a nonviscous electrolyte in an infinitely long cell. Only in the thin region adjacent to the electrodes, namely in the boundary layer, the effect of viscosity is important. These regions, close to the electrodes, are not represented in Figure 1.

Natural convection arises in electrolyte cells due to density gradients in the electrolyte. These gradients are resulting from concentration differences at the electrodes. At the cathode, the electrodeposition of metal causes a decrease of the metal-ion concentration in the vicinity of the cathode, and a natural convection upwards, as shown in Figure 1, occurs. It is assumed that the expansion of the natural convection corresponds with the hydrodynamical boundary layer.

The anodically evolved gas affects the fluid motion in the cell by two mechanisms: primarily by the buoyancy acting on the gas bubbles and secondly by a "gas-lift" effect, which can be treated as a natural convection phenomenon. The so called "gas-lift" effect occurs only if the gas bubbles were nonuniformly distributed in the electrolyte. Due to the nonuniform distribution of the bubbles, the electrolyte has a variable density. A volume element of high gas fraction has a low local density and therefore the element rises through the electrolyte.

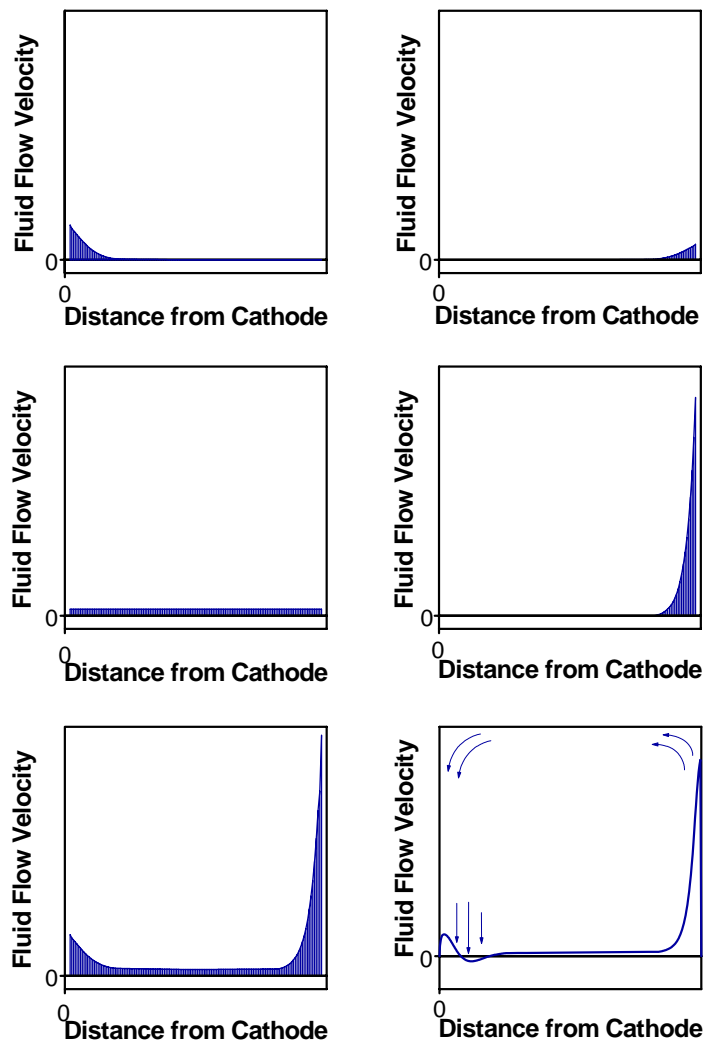


Figure 1 – Explanation of the different causes of hydrodynamic fluid flow in an aqueous electrowinning cell

The buoyancy acting on a gas bubble accelerates not only the upward flow of the gas bubbles but also the flow of the solution. Roughly the fluid moves with the rising velocity of the bubbles. The electrochemically induced gas-bubble stirring is the most

effective hydrodynamic mechanism concerning the fluid motion in the electro-winning cell.

The externally imposed fluid flow is called forced convection. An example is the electrolyte flow that is brought by pumps feeding pregnant electrolyte into an electro-winning cell.

The picture before last in Figure 1 shows an idealized velocity profile in an electro-winning cell resulting from a summation of all four schematic diagrams. An industrial electrochemical cell is not infinitely long and hence the electrolyte will, driven by the gas bubbles, recirculate. A part of the gas bubbles disengages from the electrolyte at the electrolyte surface and the electrolyte itself returns downwards in the proximity of the cathode.

## **VISUALIZATION AND QUANTIFICATION OF THE FLUID FLOW BY USING A LASER DOPPLER ANEMOMETER**

### **Experimental arrangement**

The investigations of the fluid flow were done in a laboratory electro-winning cell as shown in Figure 2. The flow direction and velocity of single volume elements were measured using a laser doppler anemometer (1).

The basic item of the experimental arrangement was the cell. At the bottom, the pregnant electrolyte flew into the cell. There were two outflows situated on both side-walls at the top of the cell. The electrodes were positioned as close as possible to the side-walls of the cell to ensure that no fluid flow could be established between side wall and electrode. The upper and the lower edge of the electrodes did not reach the free liquid surface and the cell bottom, respectively. The pregnant solution had to pass a layer of glass bulbs to realize a laminar inflow of the electrolyte. The cell was constructed in a way that the anode-cathode-spacing could be set on 15 mm and 30 mm.

The electrolyte-flow was realized by a pump and a flow regulation system. For this investigation, the change of electrolyte for the entire cell volume was achieved within two hours, which is common industrial practice. All the experiments were carried out with 2.0M  $\text{CuSO}_4$  solution with plane steel cathodes and lead-silver anodes. The amount of free acid was 165g  $\text{H}_2\text{SO}_4$ /l, and 40mg  $\text{Cl}^-$ /l were used as inhibitor. The electrolyte temperature was constantly set to 50°C. To maintain this temperature, the storage tank of the pregnant solution was put into heated water and the electrolyte flow was additionally heated by a flow heater. According to the applied current density, a certain amount of  $\text{Cu}(\text{OH})_2$  was put into the storage tank every hour to ensure that the solution would not become poor in copper. Otherwise, hydrogen ions get reduced and

hydrogen is formed on the cathode surface. The electrodes were connected to an external current circuit, which consisted of a power supply, a voltmeter and an ammeter.

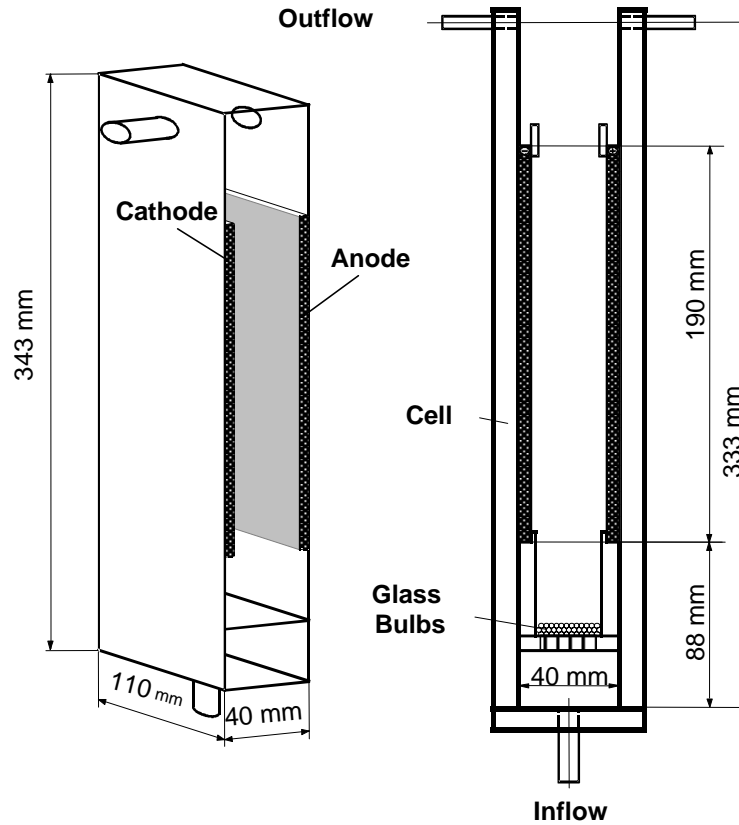


Figure 2 – Electrowinning cell

### Quantification

The measured velocity profile is approximated by five lines (Figure3). The points of intersection  $K_1$ ,  $K_2$ ,  $K_3$  and  $A$  indicate a change in the hydrodynamic mechanism. Until  $K_1$ , the natural convection is in close vicinity to the cathode predominates. According to the assumption that the thickness of the hydrodynamical boundary layer and the expansion of the natural convection is the same, the comparatively small distance  $l_{k1}$  between the cathode-surface and  $K_1$  is the hydrodynamic boundary layer.

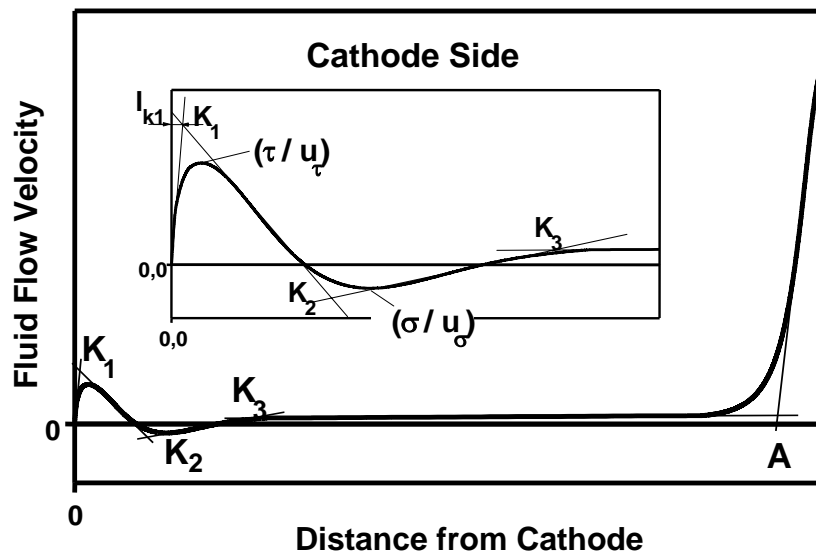


Figure 3 – Hydrodynamic characteristic

Between K<sub>1</sub> and K<sub>3</sub>, mixed convection is prevalent. The fluid flow is mainly affected by the electrochemically induced gas stirring but also by the natural convection and the forced convection. In the bulk of the electrolyte, the fluid flow is predominantly determined by turbulent eddies and the external imposed fluid circulation.

$u_{\tau}$  is the maximal positive velocity achieved nearby the cathode,  $\tau$  means the distance from the cathode at which the maximal positive velocity is located.  $u_{\sigma}$  is the maximal negative velocity imposed by the downward fluid flow. The distance between the cathode surface and the maximal negative velocity is given by  $\sigma$ .

Measurements were done for different current densities and different electrode spaces in several electrode heights (2). As an example, Figure 4 shows the flow velocity distribution using 200 A/m<sup>2</sup> current density and 30 mm electrode spacing.

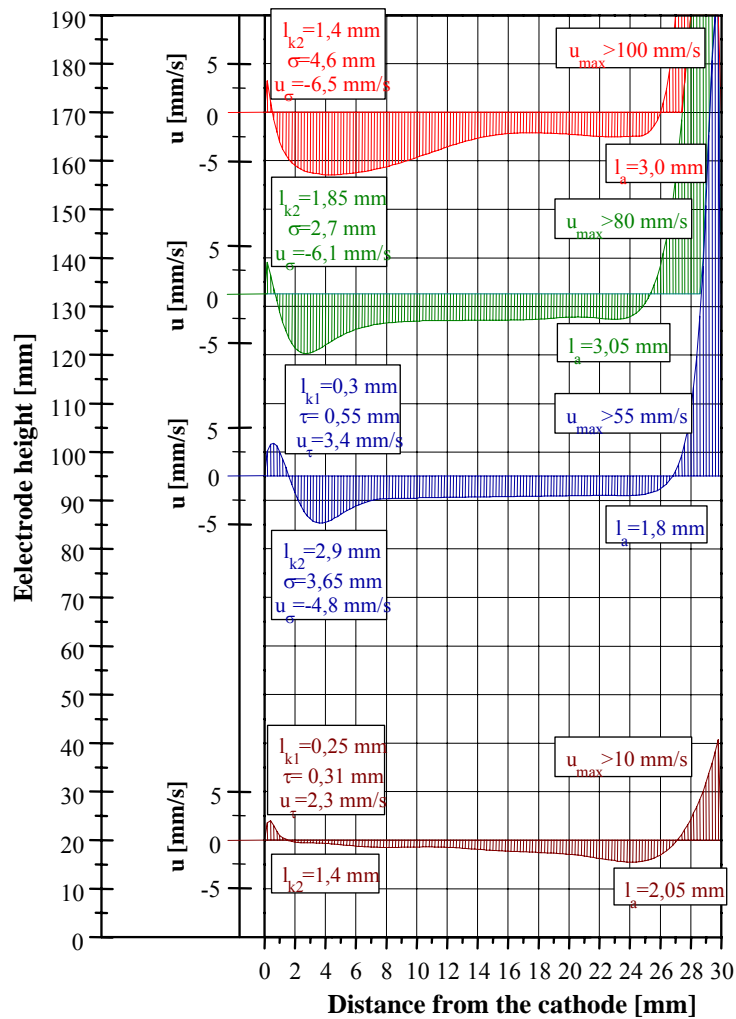


Figure 4 – Flow velocity distribution

At the upper end of the cathode, the downward fluid flow velocity of -6,45 mm/s is the most negative. With decreasing distance to the lower edge of the cathode, the downward flow reaches more positive velocities. At the electrode-height of 20 mm there is no more maximal negative velocity on the cathode-side imposed by the gas bubble driven downward fluid flow. At the anode-side, the raising velocity increases with the height. At the anode height of 170 mm, the fluid velocity of 100 mm/s is ten times the velocity of that at the bottom part of the cell.

Cause of the intensive gas stirring in the upper part of the cell the hydrodynamic boundary layer gets diminished. In this region, the mass-transport conditions are therefore improved. This highly turbulent upper zone corresponds to the section of high gas bubble concentration. Below this region, the hydrodynamic boundary layer has its largest expansion. Due to the high pressure gradient in the hydrodynamic boundary layer, a separation of this layer occurs under formation of eddies, as shown in Figure 5. The boundary-layer flow is completely turbulent in this section.

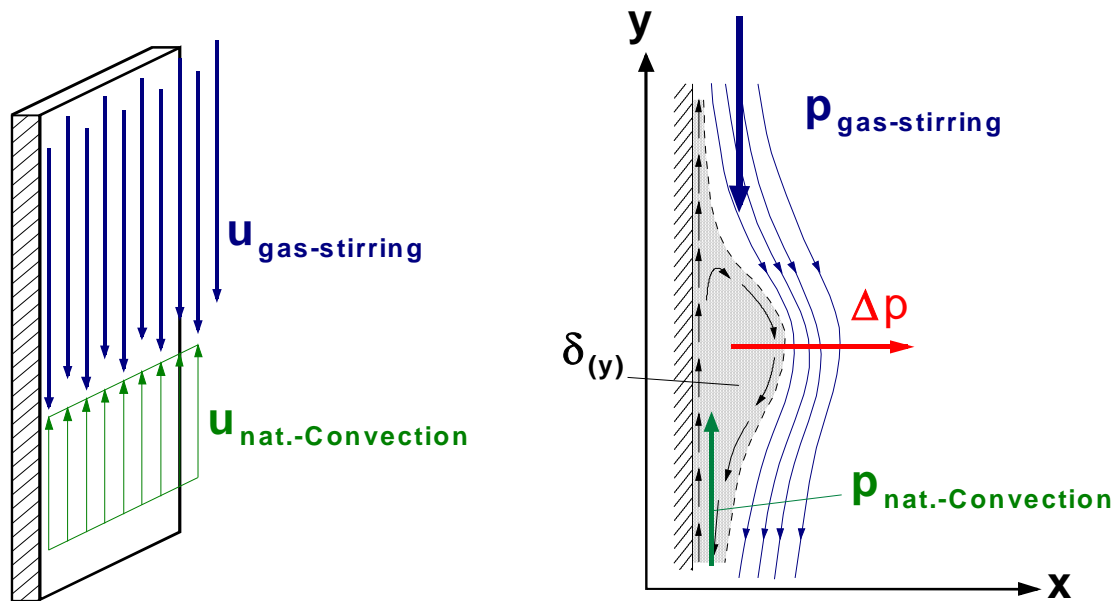


Figure 5 – Separation of the boundary layer

The height distribution of the void fraction and of the local mass-transfer is documented in Figure 6. The void fraction data were obtained by the LDA. Assuming influence of the relative gas bubble volumina onto the mass transfer, a rough estimation of the local mass transport coefficient is given (3).

The local mass-transfer coefficient increases with the distance from the lower edge of the electrode. The enhancement is due to the accumulation of rising bubbles which causes more intense fluid flow resulting in an acceleration of the mass transport. At an electrode height of 20 mm, the relative gas bubble volume is 0,9 % and the calculated value of the local mass transport velocity is 11,82 E-03 mm/s. For the electrode height of 170 mm and an experimentally determined void fraction of 13 %, the mass transport coefficient gets enhanced to 30,66 E-03 mm/s.

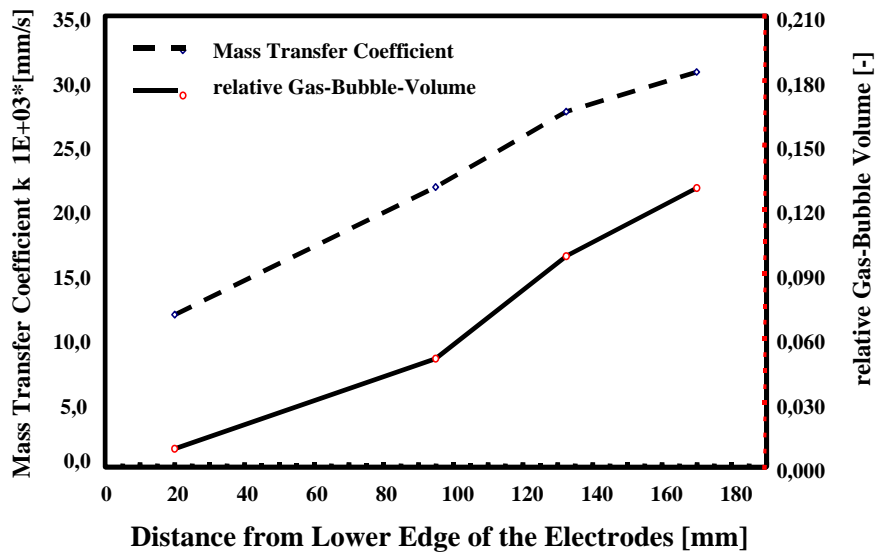


Figure 6 - Height distribution of the void fraction and of the local mass-transfer coefficient

## Visualization

The departure diameter of oxygen bubbles is about  $50 \mu\text{m}$ . The bubbles subsequently grow as they absorb oxygen from the supersaturated electrolyte and as a result of coalescence. The largest bubbles were approximately  $0,1 \text{ mm}$  in diameter at the top of the cell. The bubble diameter generally depends on the solution composition, current density and on the electrolyte-temperature. The bubble size expands with height due to the accumulation of the gas bubbles. In the upper section, the bubble size expands abruptly and reaches the cathode. The boundary between the region containing gas bubbles and the bubble free zone in the bottom part of the cell is sharp and distinct. The rising velocity of the gas bubbles increases with the bubble diameter and consequently with the height of the anode. Due to this fact, a high electrolyte circulation with vortices occurs at the top of the cell and a strong diagonally downward flow gets established. The downward flow starts nearby the cathode and with the decreasing electrode height the fluid flow shifts into the bulk of the electrolyte. The bubble-driven downward fluid flow over the cathode dominates except for a thin layer on the cathode that moves upward due to the natural convection. The flow in the bottom part of the cell is essentially natural convection resulting from density differences caused by electrodeposition.

The visual observed flow velocity distribution corresponds to the experimentally detected velocity profiles as shown in Figure 4.

## NUMERICAL SIMULATION

At the Department of Nonferrous Metallurgy at the University of Leoben, Austria, fluid flow simulations of several reactors for the nonferrous metallurgy were investigated using the CFD-code FIRE® (computational fluid dynamics). Among other things, the fluid flow field of a copper refining cell was calculated. A closer look was done to the influence of the intensity and position of in- and outlet of the forced convection on the thickness of the boundary layers and on the copper concentration profile (4).

As already mentioned before the electrochemically induced gas-bubbles stirring is the most effective hydrodynamic mechanism concerning the fluid motion, in a copper winning cell. The influence of the forced convection is weak.

To get an exact mathematical description of the fluid flow field in an electrowinning cell, it is absolute necessary to look separately at both phases, the electrolyte and the oxygen bubbles. Therefore a two-phase-model is used.

### The two fluid model

The basic idea of the two-fluid model is the coexistence of two different fluids, for example liquid and gas. Both fluids, called phases, are treated separately in Eulerian manner (5). Consequently for each phase a continuity and momentum equation is solved. Since isothermal flow is assumed no energy equation is calculated. The interaction between gas and liquid is realized by source terms occurring on the right hand side of the corresponding equations. The quantity representing the amount of a particular phase  $k$  at a certain location is called "volume-fraction  $\alpha_k$ ". Its gives information about the distribution of phase  $k$  in the flow field.

The governing equations for adiabatic two-phase flow write as follows:

Continuity for phase  $k$ :

$$\frac{\partial}{\partial t}(\alpha_k \rho_k) + \nabla \cdot (\alpha_k \rho_k \mathbf{u}_k) = \Gamma_k, \quad (1)$$

Momentum equation for phase  $k$ :

$$\frac{\partial}{\partial t}(\alpha_k \rho_k \mathbf{u}_k) + \nabla \cdot (\alpha_k \rho_k \mathbf{u}_k \mathbf{u}_k) = -\alpha_k \nabla p + \nabla \cdot \alpha_k \mathbf{t}_k + M_k + \alpha_k \rho_k \mathbf{g} \quad (2)$$

where  $t_k = \rho_k \mu_k (\nabla \cdot \mathbf{u}_k + \nabla \cdot \mathbf{u}_k^t)$  represents the stress tensor containing laminar and turbulent stresses. To account for turbulence effects, the  $k,\varepsilon$ -model is used for the liquid phase. The turbulence level of the gas phase is assumed to equal the continuous phase turbulence quantities.

Furthermore, the kinematic constraint has to be fulfilled:

$$\alpha_1 + \alpha_2 = 1 \quad (3)$$

Since mass transfer from the liquid phase (electrolyte) to the gas phase (oxygen) just occurs at the electrodes and not in the inner flow regime of the electrolytic cell, the mass transfer term  $\Gamma_k$  in Equation 1 is zero.

$$\Gamma_k = 0 \quad (4)$$

The phase transition at the electrodes is realized in the model by adequate boundary conditions, see section *Numerical Solution*.

The gas phase is assumed to be present as spherical bubbles of 0.05 mm in diameter. Therefore, the momentum interaction term between the phases can be modeled by the drag law of a spherical bubble:

$$M_k = c_D \frac{|\mathbf{u}_{rel}| \mathbf{u}_{rel}}{2} A \quad (5)$$

Where  $\mathbf{u}_{rel}$  is the relative velocity of the liquid and the gas phase and  $A$  is the cross-sectional area of a bubble. For the drag coefficient  $c_D$  the following relation is used (6).

$$c_D = \frac{24}{\text{Re}_p} (1 + 0.15 \text{Re}_p^{0.687}) \quad (6)$$

The unknowns of the two-phase flow are the volume-fractions  $\alpha_1$  and  $\alpha_2$ , the velocities  $\mathbf{u}_1$  and  $\mathbf{u}_2$  and the pressure in the fluid. An equation for the pressure is derived from the phase continuities. All equations are discretized using the finite volume method (7). The equations are solved iteratively using a SIMPLE-like algorithm (8)

## Numerical solution of the fluid flow field

The calculation of the laboratory electrowinning cell (see Figure 2) was done two-dimensionally, the cut is located in the middle plane of the cell.

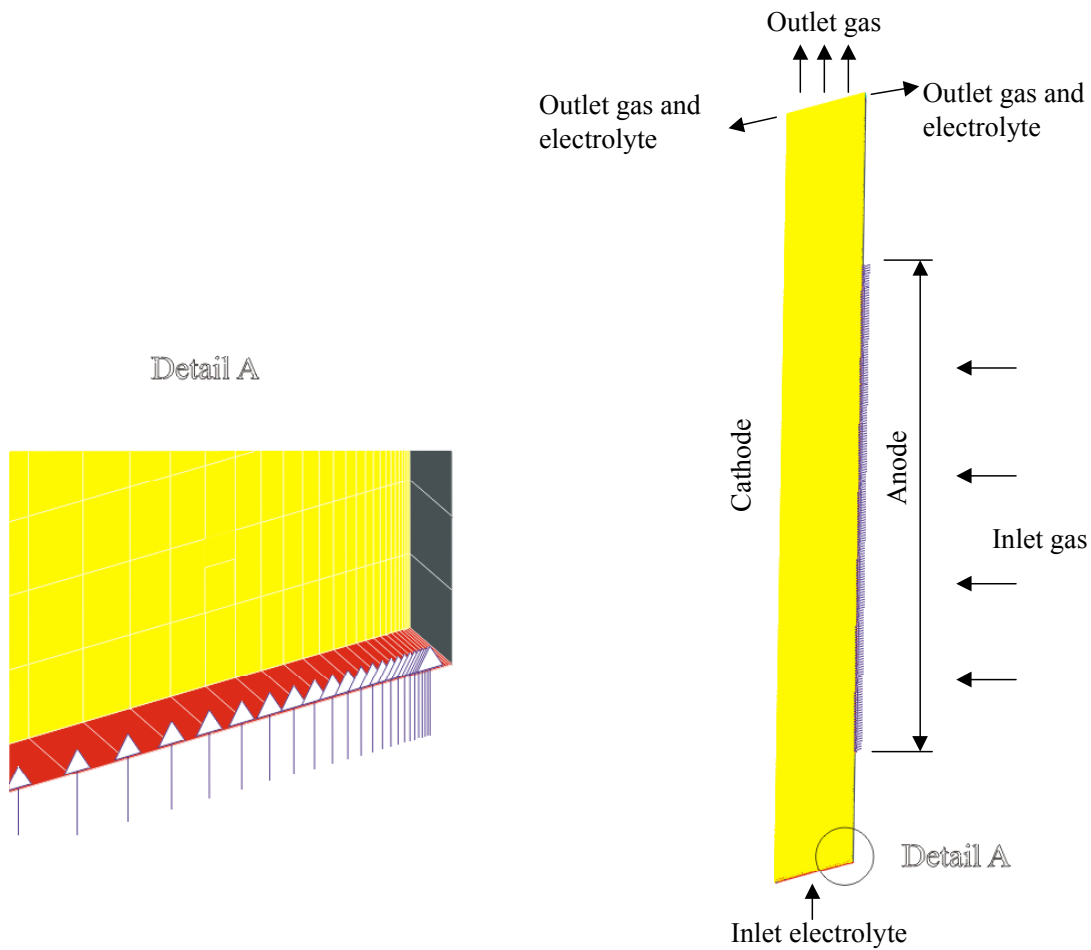


Figure 7 – Grid solution

To determine the thickness of the boundary layers and the mass transfer coefficient by the numerical method, a very fine grid solution of the geometry is

necessary. In Figure 7, the grid solution consisting of 18000 cells is shown. The thickness of the first cell-layer (the cell-layer in front of the electrodes) is approximately  $3 \text{ E-}05 \text{ m}$ .

To mode the forced convection the bottom is defined as an electrolyte inlet. The electrolyte is coming from the cell bottom and flows upwards. The chosen velocity agrees with an electrolyte exchange within two hours. As an electrolyte outlet, the first and the second cell on both sidewalls are used.

Corresponding to the cell geometry of the used laboratory cell, the anode is defined as shown in Figure 7. The bubble diameter is fixed with  $50 \mu\text{m}$ . The quantity of the anodically evolved gas is calculated as a function of the chosen current density corresponding to the Faraday's law. As a gas-outlet, the highest cell-layer as well as the electrolyte outlet is defined.

In Figure 8 the influence of the forced convection and of the bubble stirring on the velocity distribution after 0.4 seconds is shown schematically. The enlarge area is located at the upper end of the anode.

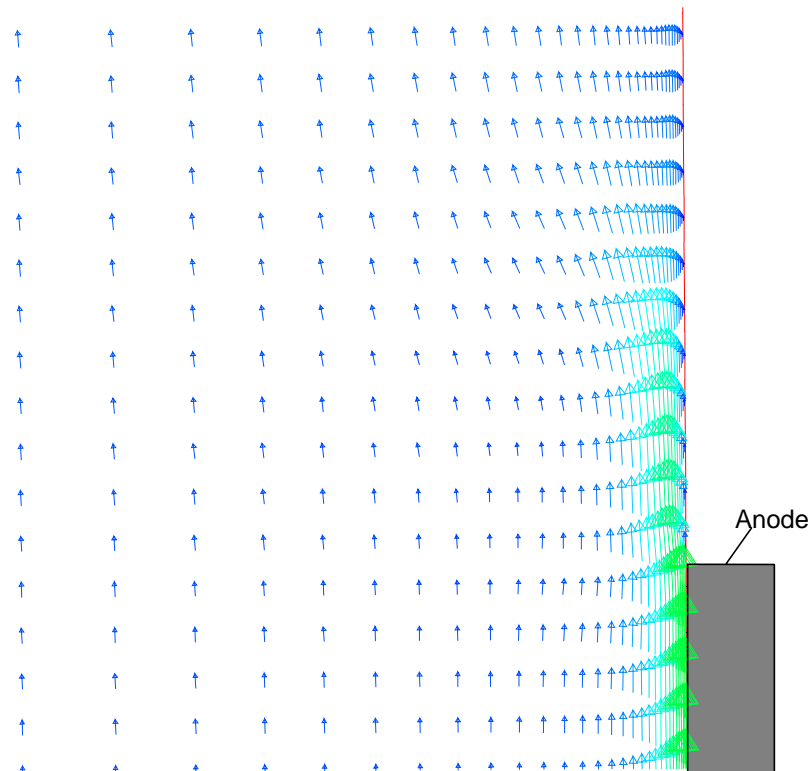


Figure 8 – Schematic velocity distribution after 0.4 seconds

The forced convection was calculated for an electrolyte exchange within two hours and the bubble stirring for a bubble diameter of 50  $\mu\text{m}$  and a current density of 1000  $\text{A}/\text{m}^2$ .

In Figure 9 the gas phase distribution after 0.4 seconds for the same area and calculation can be seen. Due to the fact that the volume fraction is known for every cell and every time the mass transfer coefficient can be calculated using the equation given in (3).

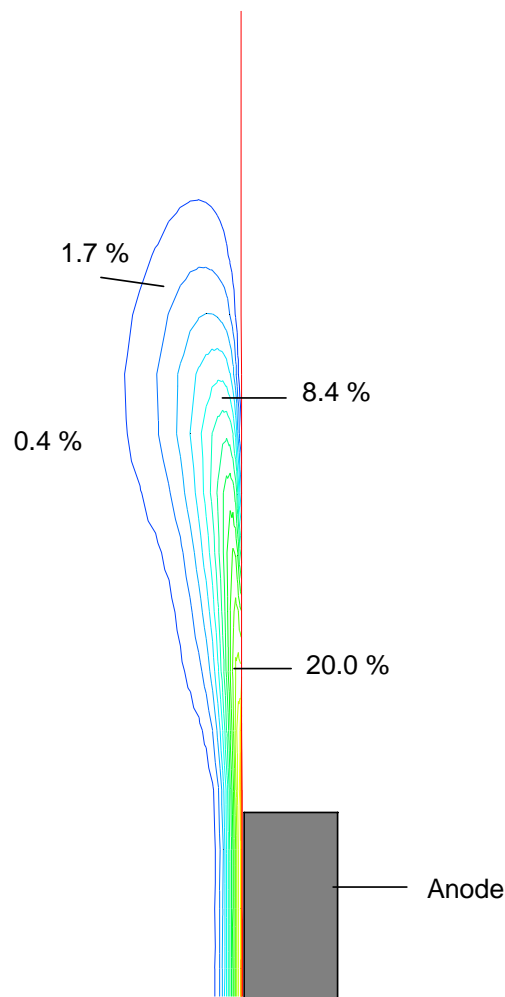


Figure 9 – Gas phase distribution after 0.4 seconds

For the calculation of the natural convection in front of the cathode an additional transport equation for the concentration of copper ions has been solved. At the cathode, the electrodeposition of metal causes a decrease of metal-ion concentration and therefore a decrease of density. The density of the electrolyte is given by a density-concentration-correlation (9) according to Equation 7

$$\rho = (841 + 1.95 c_{\text{Cu}^{2+}} + 0.48 c_{\text{H}_2\text{SO}_4}) e^{53/T} \quad (7)$$

where  $\rho$  is the density of the electrolyte in  $\text{kg/m}^3$ ,  $c_{\text{Cu}^{2+}}$  the copper concentration in  $\text{g/l}$  and  $T$  the temperature in  $\text{K}$ ,  $c_{\text{H}_2\text{SO}_4}$  was set to  $165 \text{ g/l}$  and the temperature to  $323.15 \text{ K}$ .

The copper ion concentration which is deposited at the cathode is calculated by Faraday's law as a function of current density as well as the gas bubbles evolving at the anode. By means of the Faraday's law, source terms in the transport equation for the copper concentration were defined. This method was also used to calculate the fluid flow field in a copper refining electrolysis (10).

## CONCLUSION

The fluid flow field of a copper winning electrolysis was measured using a LDA. A determination of the thickness of the hydrodynamic boundary layer and a calculation of the void fraction was done. Also a rough estimate of the mass transfer coefficient was given. The results from the LDA-measurement form the basis of the numerical simulation of the fluid flow field of an electrolysis cell. The idea and the method of a CFD-simulation is presented. First computed results point to the conclusion that a numerical simulation of a winning cell is possible.

## NOMENCLATURE

$\alpha$  ..... volume-fraction  
 $\rho$  ..... density  
 $\mathbf{u}$  ..... velocity vector  
 $p$  ..... pressure  
 $\mathbf{t}$  ..... stress tensor  
 $M_k$  ..... momentum interaction  
 $\Gamma_k$  ..... mass transfer  
 $c_D$  ..... drag coefficient  
 $Re_p$  ..... bubble Reynolds number  
 $\mathbf{g}$  ..... gravity vector

## REFERENCES

1. K. Hein, G. Hanko, A. Filzwieser and M. Stelter, "Investigation of the Hydrodynamic in a Copper Winning Electrolysis" (in German), Berg- und Hüttenmännische Monatshefte, Vol. 144, Springer Verlag, Wien, 1999, 6-13.
2. G. Hanko, K. Hein and A. Filzwieser, "Visualization and Quantification of the Fluid Flow in a Copper Electrowinning Cell" (in German), Erzmetall, Vol.52, 1999, 226-235.
3. A. Shah and J. Jorne, "Mass Transfer and Bubbles-Induced Convection in a Vertical Electrochemical Cell", Journal of the Electrochemical Society, Vol. 136, 144-158.
4. A. Lackner, K. Pachler, P. Paschen and K. Hein, "CFD-Simulation of Copper Electrolysis – a Way to a New Cell Design", CFD and Heat/Mass Transfer Modelling in the Metallurgical Industry, S. Argyropoulos, CIM, Canada, 1996, 293-304.
5. A. Drew, "Mathematical Modeling of Two-Phase Flow", Ann. Rev. Fluid Mech., Vol. 15, 1983, 261-291.
6. R. Clift, J. R. Grace and M. E. Weber, Bubbles, Drops and Particles, Academic Press, 1978.
7. J. H. Ferziger and M. Peric, Computational Methods for Fluid Dynamics, Springer 1996.
8. D. B. Spalding, The Numerical Computation of Multi-Phase Flows, Imperial College of Science and Technology, 1985.
9. J. Hotlos and M. Jaskula, "Densities and Viscosities of  $\text{CuSO}_4\text{-H}_2\text{SO}_4\text{-H}_2\text{O}$  Solutions", Hydrometallurgy, Vol. 21, 1988, 1-7.
10. A. Filzwieser, A. Lackner, K. Hein and K. Pachler, "Process Simulation of Copper Refining Electrolysis", 4<sup>th</sup> International Colloquium on Process Simulation, Espoo, Finland, 1997, 431-446.